

# Second Transfer Process Simulation I

Toyoshige Sasaki<sup>1</sup>, Takuma Onishi<sup>1</sup>, Asako Sugiyama<sup>1</sup>, Yasuo Yoda<sup>2</sup>, Takeshi Tomizawa<sup>3</sup>

<sup>\*1</sup> Analysis Technology Center, Canon Inc., Tokyo, Japan

<sup>\*2</sup> Peripherals Development Center, Canon Inc., Shizuoka, Japan

<sup>\*3</sup> Office Imaging Products Device Development Center, Canon Inc., Ibaraki, Japan

## Abstract

We have developed a numerical simulation method and used it to understand the control mechanism for separation discharges and toner scattering in the second transfer process. The second transfer process involves various materials, including paper, rollers, toner, intermediate transfer belt (ITB) and saw-like static charge eliminator. The simulation method takes into consideration electrical materials, geometric configuration and physical interaction among many factors: electric field, charge conduction, electric discharges, toner behavior, and ion flow field. The developed method was used to calculate the current characteristics, electric discharges, and toner scattering. Results showed good agreement with the experiments, and further calculation results showed that removal of electricity by static charge eliminator reduces toner scattering and separation discharges.

## Introduction

In electro-photographic systems such as printers or copiers, the intermediate transfer system comprising both a first and second transfer process is a commonly used system to achieve high quality and robust performance. Numerical simulation techniques have been applied during these processes to analyze defects in toner images<sup>[1]-[2]</sup>. Although the first transfer process has been studied extensively, the second transfer process has seldom been analyzed. During the second transfer process, interference from the paper, rollers, toner, intermediate transfer belt (ITB) and saw-like static charge eliminator causes electric discharges and toner scattering. Analysis techniques must take into consideration geometric configuration and multi-physics, which can express the complex interaction of factors: electric discharges across the air gap, ion flow from the static charge eliminator, electric conduction on materials and toner motion.

This study is intended to verify the developed numerical simulation method and to understand the control mechanism on the second transfer process using the method. Verification is carried out by comparing the calculation results and the experiment on the electric current (IV characteristics). The method helps clarify the mechanism of the static charge eliminator effecting the separation discharges and toner scattering.

## Simulation Method

Figure 1 shows the calculation flowchart, which consists of five main calculation steps: electric field, electric discharges, ion flow field, electric conduction and toner motion, the details of which are described below.

## Electric Field

Poisson's equation is used to obtain the electric potential as follows:

$$\text{div}(\epsilon \text{ grad } \phi) = -\rho \quad (1)$$

where  $\epsilon$ ,  $\phi$  and  $\rho$  are the permittivities, electric potential and charge density, respectively. The finite element method, with the following arrangement, can be used to solve them as simultaneous equations of many unknowns:

$$\iint_{\Omega} \left( \epsilon \frac{\partial N_i}{\partial x} \frac{\partial \phi}{\partial x} + \epsilon \frac{\partial N_i}{\partial y} \frac{\partial \phi}{\partial y} \right) dS = \iint_{\Omega} N_i \rho dS \quad (2)$$

where  $\Omega$  and  $N_i$  are the analysis region and the test function, respectively.

## Electric Discharges

Figure 2 is a schematic diagram of the method for calculating the electric charge transfer by electric discharges in the finite element model (FE model) from a higher- to lower-voltage surface. The threshold voltage of the electric discharges between node  $i$  and node  $j$  is subject to Paschen's law. The relationship between the high- and low-voltage surfaces is as follows:

$$\begin{cases} Q'_i = Q_i - \Delta Q_{ij} \\ Q'_j = Q_j + \Delta Q_{ij} \end{cases} \quad (3)$$

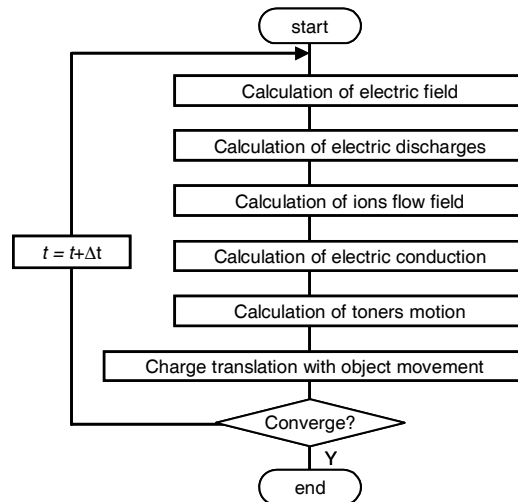


Figure 1. Simulation flowchart

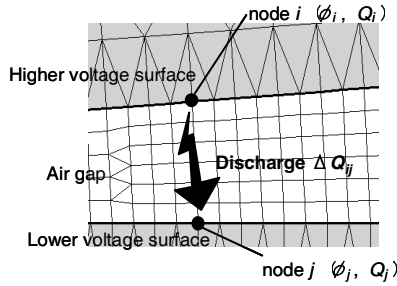


Figure 2. Schematic diagram of electric discharges

where  $Q_i$ ,  $Q_j$  and  $\Delta Q_{ij}$  are the electric charge of the high-voltage surface, electric charge of the low-voltage surface and transfer charge between the two surfaces, respectively.  $Q_i'$  and  $Q_j'$  show the values after electric discharges. The relationship between the nodes on both surfaces in terms of electric potential is as follows:

$$\phi_i' - \phi_j' = V_{pa}^{(ij)} \quad (4)$$

where  $\phi_i'$ ,  $\phi_j'$  and  $V_{pa}^{(ij)}$  are the electric potential of the high-voltage surface, electric potential of the low-voltage surface, and Paschen's voltage, respectively. The electric charge after discharging can be obtained by substituting Eqs. (3) and (4) into Eq. (2).

### Ion Flow Field

The charge transferred from the static charge eliminator is calculated, assuming that the ion flow immediately turns into a steady state at each time step. The equation for current continuity is:

$$\text{div}(\mu \rho \text{grad} \phi) = 0 \quad (5)$$

where  $\mu$  is the mobility of air. The following equation is obtained referring to the vector formula:

$$\mu \text{grad} \phi \bullet \text{grad} \rho = \frac{\mu \rho^2}{\epsilon_0} \quad (6)$$

where  $\epsilon_0$  is the permittivity of air. Taking into consideration the characteristic lines<sup>[3]</sup>, Eq. (6) can be rewritten as follows:

$$\frac{d\rho}{dt} = -\frac{\mu \rho^2}{\epsilon_0} \quad (7)$$

$\rho$  can be obtained by solving Eq. (7).

$$\rho = \frac{1}{\frac{1}{\rho_0} + \frac{\mu t}{\epsilon_0}} \quad (8)$$

where  $\rho_0$  and  $t$  are the electric charge density at the starting point of the characteristic line and the time from the starting point, respectively.

### Electric Conduction

The following equation is formed by applying Ohm's law to the law of conservation of electric charge.

$$\frac{\partial \rho}{\partial t} = \text{div}(\sigma \text{grad} \phi) \quad (9)$$

where  $\sigma$  is the electric conductivity. The finite element equation is as follows:

$$\iint_{\Omega} N_i \frac{\partial \rho}{\partial t} dS = - \iint_{\Omega} \left( \sigma \frac{\partial N_i}{\partial x} \frac{\partial \phi}{\partial x} + \sigma \frac{\partial N_i}{\partial y} \frac{\partial \phi}{\partial y} \right) dS \quad (10)$$

The value at the next time step is as follows:

$$\iint_{\Omega} N_i \rho^{<k+1>} dS = \iint_{\Omega} N_i \rho^{<k>} dS + \iint_{\Omega} N_i \frac{\partial \rho^{<k>}}{\partial t} \Delta t dS \quad (11)$$

where  $\rho^{<k+1>}$  and  $\rho^{<k>}$  are the “k+1”th and “k”th electric charge density, respectively, and  $\Delta t$  is the time interval. The electric potential after electric conduction can be obtained by substituting Eq. (11) into Eq. (2).

### Toner Motion

The following equation is formed on the assumption that the shape of the toner particle is a complete sphere and the charge is concentrated in the center.

$$F(t) = Q_T E(t) \quad (12)$$

where  $F$ ,  $Q_T$  and  $E$  are the force of the toner particles, the charge and the electric field at the center.

For calculating the motion of the toner, equations of motion are applied as shown below:

$$\begin{cases} v(t + \Delta t) = v(t) + \frac{F(t)}{m} \Delta t \\ x(t + \Delta t) = x(t) + v(t) \Delta t + \frac{1}{2} \frac{F(t)}{m} \Delta t^2 \end{cases} \quad (13)$$

where  $v$ ,  $x$  and  $m$  are the velocity, location, and weight of the toner particles, respectively. The location of the toner at the next step can be calculated by solving Eq. (13). For collision between toner particles and other objects, the hard sphere collision theory is applied (cf. Conservation of Momentum).

## Results and Discussion

### Simulation Model

Figure 3 shows the FE model used for verifying the numerical simulation method. This model consists of a facing roller, intermediate transfer belt (ITB), transfer roller, paper, and static charge eliminator. The ITB winds around the facing roller, the paper is nipped between the ITB and the transfer roller, and the static charge eliminator is kept grounded (GND) and located at the outlet of the nipped region. Since the facing roller is already a perfect conductor material, it is not shown in Figure 3. The facing roller is maintained as GND, and the electric potential ( $V_T$ ) of the shaft of the transfer roller varies between 1 and 4 kV.

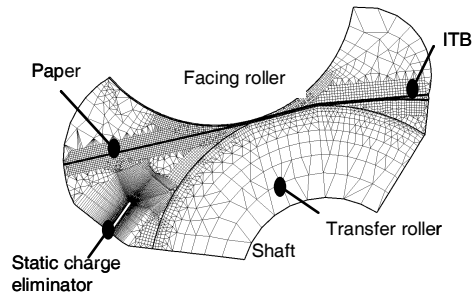


Figure 3. Simulation FE model for verification

#### IV Characteristics

Figure 4 shows the calculations and experiments performed to obtain the relationship between  $V_T$  and the two currents: one flowing to the shaft of the transfer roller ( $I_T$ ) and the other flowing to the static charge eliminator ( $I_E$ ). The results found that the calculations coincide with the experiments in terms of threshold voltage and current increasing rate.

#### Electric Discharges

The electric discharges behavior near the outlet of the nipped region with the static charge eliminator is shown in Figure 5.

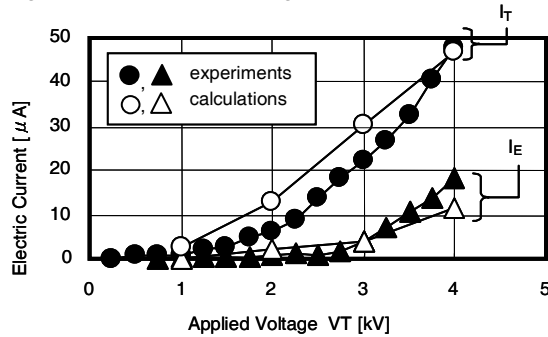


Figure 4. IV characteristics

Figure 5 (a) and (b) are, respectively, experiments and calculations varying from 1 to 4 kV in four grades. The contour shows the distribution of electric potential and the black lines from the tip of the eliminator trace the ion flow. As for the discharges between the ITB and facing roller, the calculations and experiments were accorded a discharges starting at 3 kV. Notice that the separation discharges between the ITB and the paper in both the calculations and the experiments reaches the maximum at the condition of applying 1 kV, which is the weakest supply voltage. As can be seen from Figure 5, by supplying a higher voltage, the ion flow expands up to the nipped region, and the charge is removed from around the paper by the nipped region. This is due to the increase in voltage of the transfer roller and the change in direction of the electric field near the tip of the eliminator from the paper toward the nipped region. By supplying a higher voltage, the eliminator removes the charge on the paper at the nipped region. As a result, the discharges between the paper and ITB decreases.

#### Toner Scattering

Figure 6 shows layers of the toner status at a point about 6mm down from the nipped region. The calculations qualitatively agree with the experiments in the following respects: the toner at

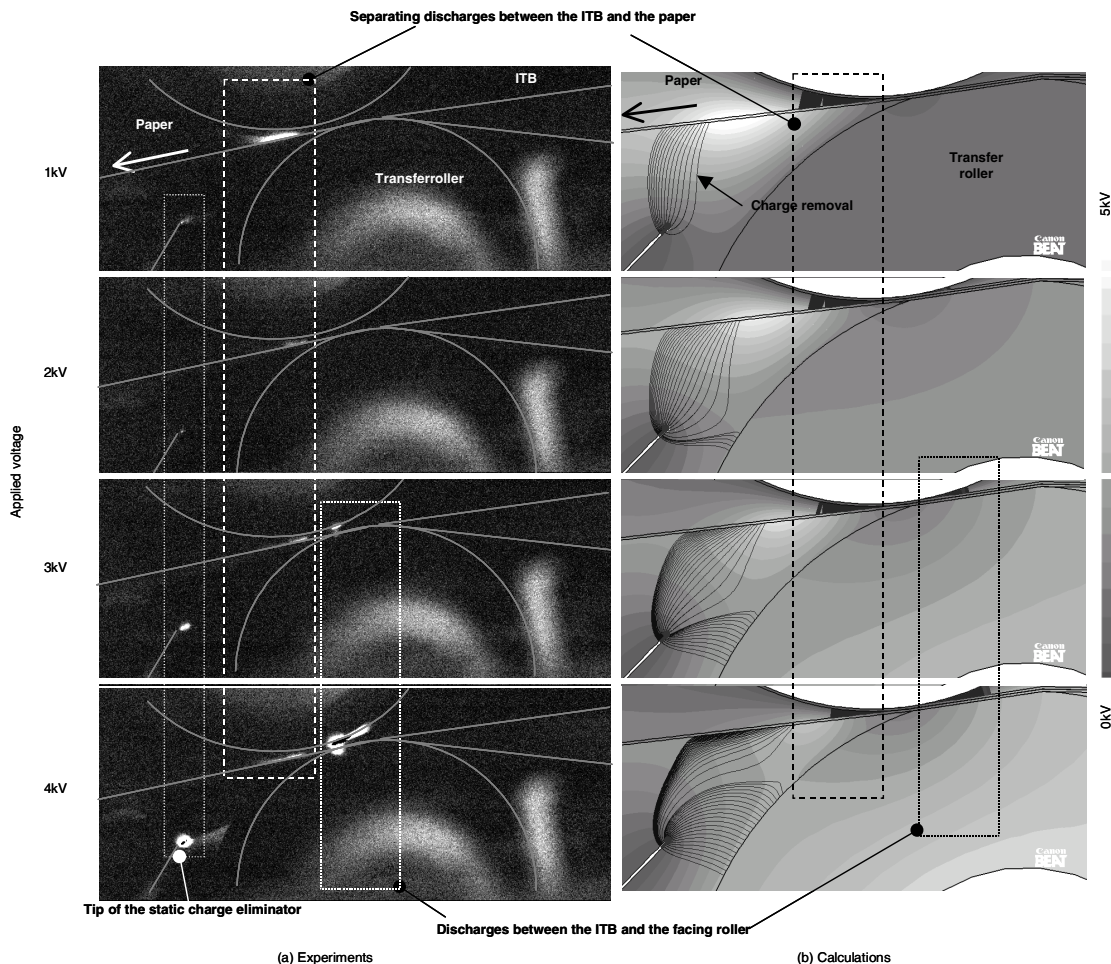


Figure 5. Comparison of electric discharges with experiments and calculations

$V_T = 2$  kV without the eliminator completely scatters, the toner at  $V_T = 2$  kV with the eliminator still scatters but at a reduced rate, and the toner at  $V_T = 3$  kV with the eliminator has almost no scattering.

Figure 7 shows the trajectory of scattering toner at  $V_T = 2$  kV without the eliminator. In this figure, the contour illustrates the distribution of electric potential, and the black lines trace the scattering toner. It is clear from this figure that the electric potential gradient from the image area to non-image area is the cause of scattering toner. An analysis of Figure 7 reveals the following interesting facts. When applying 2 kV, there is not enough positive charge on the paper in the image area to neutralize the negative charge from the toner. Thus, the voltage on the image area is lower than that on the non-image area. Consequently, the toner on the image area scatters over the non-image area. However, an electric charge eliminator added to this system will get rid of the positive charge on the non-image area, and the electric potential gradient from the image area to the non-image area will weaken, thus reducing the scattering. In addition, by shifting the voltage to 3 kV, the paper in the image area will have enough positive charge to neutralize the negative charge created by the toner, and scattering will not occur.

## Conclusion

A numerical simulation method was developed and applied to the analysis of the second transfer process. It was found that ion flow from the static charge eliminator affects the behavior of separation discharges and toner scattering.

In our next study, we intend to investigate problems that may occur during sheet transportation by further developing this method.

## References

- [1] M. Kadonaga, T. Takahashi and H. Iimura, Numerical Simulation of Toner Movement in a Transfer Process, IS&T's NIP21, pg.594 (2005).
- [2] S.Aoki, M. Sukesako and M. Kadonaga, A Numerical Simulation Method of Toner Transfer Considering Voltage Distribution of Transfer Belt, Proc.NIP23, pg.77 (2007).
- [3] J.L. Davis and J.F. Hoburg, HVDC transmission line computations using finite element and characteristics methods, J. Electrostat., 18, pg.1 (1986).

## Author Biography

Toyoshige Sasaki received his B.S. and M.S. degrees from Waseda University, Japan in 1982 and 1984, respectively. He joined Canon in 1984 and has been engaged in the development of electromagnetic devices such as magnetic recording media, actuators, and electro-photography by using numerical simulation.

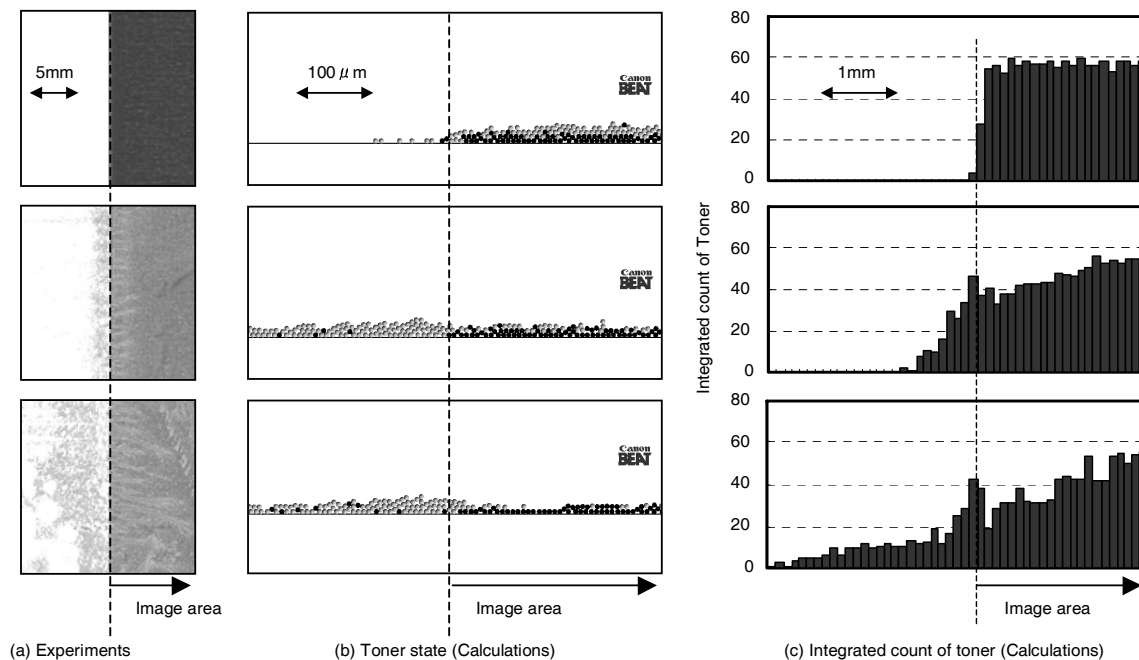


Figure 6. Toner scattering (upper:  $V_T = 3$  kV with the eliminator; middle:  $V_T = 2$  kV with the eliminator; lower:  $V_T = 2$  kV without the eliminator)

3kV

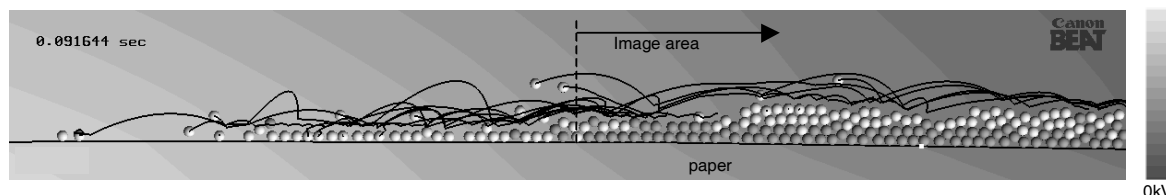


Figure7. Trajectory of scattering toner ( $V_T = 2$  kV without the eliminator)